GeoConvention 2014 FOCUS | adapt refine sustain

Linear Solid/Fluid Seismic Model for Heavy-Oil Related Media

Igor B. Morozov and Wubing Deng
University of Saskatchewan

Summary

The existing approaches to modeling seismic waves in attenuative media are based on time-dependent moduli and the quality factor (Q). In numerical algorithms, these properties are usually implemented by the Generalized Standard Linear Solid (GSLS), which is often illustrated by combinations of elastic and damping mechanical elements arranged in 'Maxwell's bodies'. However, although the concepts of Q and GSLS are usually thought to be very general, neither of them covers all cases of practical importance. In particular, the GSLS appears inadequate for fluids, fluid/solid mixtures, saturated porous rocks, and generally cases of low *Q* and transitional solid-fluid behaviour, such as bitumen-rich rocks.

Here, we propose a broader class of rheologies that we call the General Linear Solid (GLS). The GLS is rigorously described by using the macroscopic continuum Lagrangian mechanics. Conventional spring-dashpot diagrams can be used to represent the structure of the Lagrangian model. The GLS rheology includes viscous solids, fluids, fluid-saturated porous rocks as well as the GSLS and numerous more complex cases. The model also offers straightforward extensions, such as to thermoelasticity and nonlinear elasticity, viscosity, and plasticity. GLS equations of motion take the form of differential matrix equations, and finite-difference schemes can be readily derived for numerical simulations in such media. The model is illustrated by modeling recent observations of low-frequency P-wave viscoelasticity in bitumen sands.

Introduction

To explain the attenuation of seismic waves, the inelasticity of the Earth is usually parameterized by the quality factor (*Q*) attributed to materials. The effects of *Qs* and *Q*-contrasts on wave propagation are discussed in many 'classic' and recent studies (e.g., Lines et al., 2014). Numerical modeling of seismic wavefields is also commonly based on the *Q* phenomenology. In modeling, certain *Q*(*f*) spectra (usually, $Q(f) \approx \text{const}$) are commonly achieved by constructing internal variables ('memory' variables; e.g., Zhu et al., 2013) or mechanical models of the medium, such as the Generalized Standard Linear Solid (GSLS; Liu, 1976; Figure 1).

The *Q* and GSLS models are often viewed as almost universal, and they are represented in almost all seismic-waveform modeling software. Nevertheless, these models are in fact overly restrictive and may be inadequate for bitumen-rich rocks and heavy oil. This limitation occurs because the model in Figure 1 lacks both fluid viscosity (a damper placed parallel to element *M*) and poroelastic friction (discussed below). However, viscous and pore-fluid type internal-friction mechanisms are likely important for the bitumen.

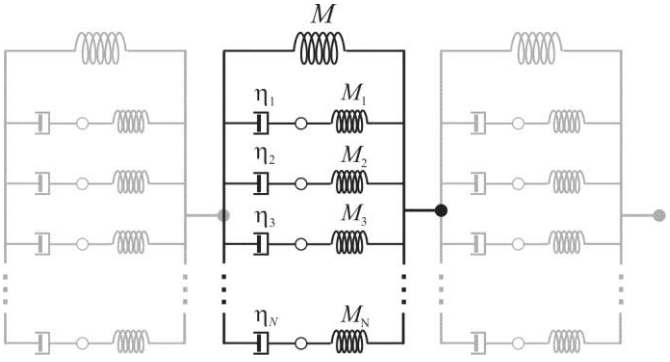

Figure 1. Generalized Standard Linear Solid (GSLS; black) model commonly used to implement attenuation and memory variables in finite-difference algorithms. Parameters *M* are moduli (observable and internal) and η denote the internal viscosities of *N* Maxwell's bodies. White circles are hidden internal variables.

In this paper, we try formulating a much more

general theoretical model that would be compatible with the physics of seismic wave attenuation in various media. The internal friction in materials occurs not because of a '*Q*' but through a variety of specific physical mechanisms, such as viscosity, pore fluid flows, or thermoelasticity. It is important to try explaining the effects of attenuation directly in terms of such physical quantities rather than by empirical Q(*f*) spectra or effective moduli.

For a first-principle physical description of wave-propagating media, continuum Lagrangian mechanics (Landau and Lifshitz, 1986) is the most complete, rigorous, and at the same time assumption-free and simple language. This language allows naturally incorporating all known mechanisms of internal friction and considering new ones. Note that Biot's (1956) model of wave propagation in saturated porous rock is also based on Lagrangian formulation. This approach also explains the meanings of the conventional spring-dashpot diagrams commonly used to illustrate the viscoelasticity (e.g., Lakes, 2009) and reveals the intricacies of the mathematical tools used for modeling attenuation, such as the finite-difference memory variables (Deng and Morozov, 2013).

Below, we describe a broad class of second-order rheologic laws that we call the General Linear Solid (GLS). This class combines and generalizes the Newtonian fluid, the conventional GSLS, and models of saturated porous rock (Biot, 1956; Bourbié et al., 1987). We show that by combining such models in a common matrix formalism, rigorous and realistic analytical and finite-difference models are obtained. These models should be useful for application to strongly-attenuating, fluid-rich or fluid-like media.

Theory

Lagrangian continuum mechanics

Lagrangian mechanics is based on the Hamiltonian variational principle of stationary action (Landau and Lifshitz, 1986). Unfortunately, this approach is still poorly utilized in seismology, perhaps with the exception of poroelasticity (Biot, 1956). The principle of this approach consists in analysing the functional form of its Lagrangian density as a function of mutually independent displacements and velocities. For an isotropic medium, the Lagrangian density is a combination of two second-order, rotational invariants of the strain tensor: $I_1 = (\varepsilon_{kk})^2$ and $I_2 = \varepsilon_{ij}\varepsilon_{ij}$. Two useful forms for the Lagrangian density are (*e.g.*, Landau and Lifshitz, 1986):

$$L\{\mathbf{u}, \dot{\mathbf{u}}\} = \frac{\rho}{2}\dot{u}_i\dot{u}_i - \frac{\lambda}{2}\varepsilon_{kk}\varepsilon_{ll} - \mu\varepsilon_{ij}\varepsilon_{ij} \equiv \frac{\rho}{2}\dot{u}_i\dot{u}_i - \frac{K}{2}\Delta^2 - \mu\tilde{\varepsilon}_{ij}\tilde{\varepsilon}_{ij}, \tag{1}$$

where *i* = 1, 2, or 3 denotes the spatial dimensions, $\Delta \equiv \varepsilon_{kk}$ is the volumetric strain, $\tilde{\varepsilon}_{ij} \equiv \varepsilon_{ij} - \Delta\delta_{ij}/3$ is the deviatoric (pure shear) strain, and summations over all pairs of repeated indices are assumed. Parameters λ and μ are the (isothermal) Lamé elastic constants, $K \equiv \lambda + 2\mu/3$ is the bulk modulus, and ρ is the mass density. All medium parameters (ρ, λ, K and μ) are real-valued and time- and frequency-independent. To obtain a fluid, we only need to drop the shear-energy part in (1), which can be done by setting $\mu = 0$.

The internal mechanical friction (fluid or solid viscosity) is described by a similar function called the dissipation function or pseudo-potential, *D*. Unlike the elastic energy, *D* principally depends on the strain rates. If we consider an isotropic medium and assume no internal variables such as those of pore fluids, then similarly to expression (1), the pseudo-potential *D* equals:

$$D\{\mathbf{u}, \dot{\mathbf{u}}\} = \frac{\eta_\lambda}{2}\dot{\Delta}^2 + \eta_\mu\dot{\tilde{\varepsilon}}_{ij}\dot{\tilde{\varepsilon}}_{ij} \equiv \frac{\eta_\Delta}{2}\dot{\Delta}^2 + \eta_\varepsilon\dot{\tilde{\varepsilon}}_{ij}\dot{\tilde{\varepsilon}}_{ij}. \tag{2}$$

This viscosity law ('rheology') corresponds to the Naviér-Stokes equations for a Newtonian (compressible) fluid or to linear viscosity in a solid (Landau and Lifshitz, 1986).

Spring-dashpot diagrams

Mechanical properties of viscoelastic materials are often illustrated by arrangements of interconnected strings and dashpots (e.g., Lakes, 2009). It is usually noted that such diagrams are to be understood

not as construction of materials but only as implementations of certain causal stress-strain time dependences (*ibid*). In particular, different configurations of springs and dashpots can lead to identical strain-stress relations, but only the latter are considered important for deriving the wave motion.

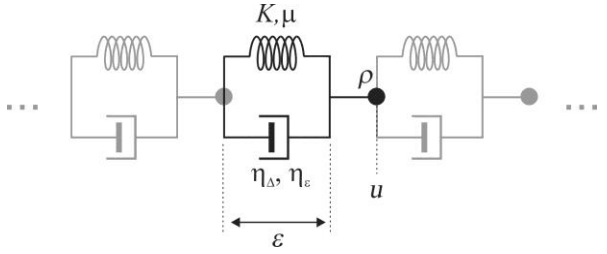

Figure 2. Voigt spring-dashpot model (black) illustrating the structure of the Lagrangian (eq. (1)) and dissipation function (eq. (2)) for a Newtonian solid.

However, we argue the contrary, namely that the spring-dashpot systems are actually *more important* than the time-dependent strain-stress relations they implement. From the viewpoint of Lagrangian mechanics, these diagrams graphically represent the selection of observable and internal variables and the functional forms selected for *L* and *D*. For example, the Voigt body in Figure 2 depicts the structure of the Lagrangian (1) and dissipation function (2) for a Newtonian solid. The black dot in Figure 2 indicates the state variable (**u**) with the corresponding kinetic-energy term (indicated by density ρ), the spring represents the elastic-energy terms in *L*, and the dashpot illustrates the quadratic function *D*. The spring and the dashpot are connected in parallel, meaning that they share a common strain tensor, **ε** (Figure 2). Note that in finite-difference modeling of anelastic solids, implementations of memory variables can always be described by a GSLS (e.g., Zhu et al., 2013), and therefore memory variables also follow from the selected spring-dashpot arrangements (Deng and Morozov, 2013).

General Linear Solid rheology

Thus, *all* existing finite-difference models of solid media can be fully described by Lagrangian mechanics. Let us therefore consider a more general mechanical system with *N* internal variables, which we call the General Linear Solid (GLS). Similarly to eqs. (1) and (2), we only use second-order forms for the kinetic energy, elastic energy, and dissipation function:

$$\begin{cases} L = \frac{1}{2}\dot{u}_{Ii}\rho_{IJ}\dot{u}_{Ji} - \frac{1}{2}\Delta_I\lambda_{IJ}\Delta_J - \varepsilon_{Iij}\mu_{IJ}\varepsilon_{Jij}, \\ D = \frac{1}{2}\dot{u}_{Ii}d_{IJ}\dot{u}_{Ji} + \frac{1}{2}\dot{\Delta}_I\eta_{\lambda IJ}\dot{\Delta}_J + \dot{\varepsilon}_{Iij}\eta_{\mu IJ}\dot{\varepsilon}_{Jij}. \end{cases} \tag{3}$$

where the density (ρ), moduli (λ and μ), and viscosities (η_λ and η_μ) are matrix properties, the upper-case subscripts *I*,*J* = 0 correspond to the observable deformation parameters (displacement and strain), *I*,*J* = 1,… *N* enumerate the internal variables, and the lower-case subscripts *i*,*j* = 1,2,3 denote the spatial coordinates. An additional 'damping' matrix **d** is added to represent the mechanical friction caused by interactions between the components of the system. This term is constructed completely similar to the kinetic energy in *L*. Relations (3) can be expressed by using symmetric matrices ρ, **K**, μ, **d**, η_λ, and η_μ in the *N* + 1 dimensional space of state variables. Because the selection of internal variables can be relatively arbitrary, it is convenient to perform it so that it diagonalizes one of these matrices. Therefore, this medium generally requires $(N+1)(5N+12)/2$ mechanical parameters for its characterization.

The only property specified by the GLS relations (3) is that its responses to all deformations and/or deformation rates are linear. In terms of the diagrams similar to Figure 2, the GLS would have each variable connected to all others by dashpots and springs. A GSLS (Figure 1) would be obtained by setting the viscosities corresponding to the observable deformation equal zero: $\eta_{\lambda 00} = \eta_{\mu 00} = 0$. A Maxwell's solid is obtained by additionally setting $\lambda_{00} = \mu_{00} = 0$ and taking *N* = 1. A Voigt solid is obtained by setting N = 0 (no internal variables). Finally, by setting the shear rigidity matrix $\boldsymbol{\mu} \equiv 0$, the Voigt solid becomes a Newtonian fluid with respect to seismic waves.

Another restriction of relations (3) is that the deformations associated with different variables and the velocity-related damping **d** are considered not coupled to each other. This restriction is only made for

simplicity and can of course be lifted if needed.

Equations of motion

The equations of motion for the field resulting from functions (3) are (Landau and Lifshitz, 1986):

$$\boldsymbol{\rho}\ddot{\mathbf{u}}_i = -\mathbf{d}\dot{\mathbf{u}}_i + \partial_j \boldsymbol{\sigma}_{ij}\,, \tag{4}$$

where the strain-related (elastic and viscous) stress tensor equals:

$$\boldsymbol{\sigma}_{ij} = \boldsymbol{\lambda}\boldsymbol{\Delta}\delta_{ij} + 2\boldsymbol{\mu}\boldsymbol{\varepsilon}_{ij} + \boldsymbol{\eta}_\lambda\dot{\boldsymbol{\Delta}}\delta_{ij} + 2\boldsymbol{\eta}_\mu\dot{\boldsymbol{\varepsilon}}_{ij}\,. \tag{5}$$

The general form of expressions (3) leads to an important observation about anelastic systems. Only for matrices $\boldsymbol{\rho}$ containing a single nonzero element ρ_{00}, the behavior of internal variables is completely localized in space and reduces to memory integrals in time (Deng and Morozov, 2013). For non-trivial density matrices, the internal variables interact spatially (through terms containing λ_{IJ}, μ_{IJ}, $\eta_{\lambda IJ}$, and $\eta_{\mu IJ}$ in (3)) and lead to additional wave modes. Therefore, simply specifying the desired $Q(f)$ function at every point and approximating it by a certain number of internal variables is generally insufficient for a describing an inelastic solid or fluid. For example, on the free surface of an anelastic body, one has to also formulate the boundary conditions for all internal variables u_J, with $J = 1,\ldots, N$. This situation is well known in poroelasticity, where special boundary conditions for fluid flow are required.

Correspondence principle

For a harmonic oscillation at angular frequency ω, all variables $\mathbf{u}$ are proportional to $\exp(-i\omega t)$, and eqs. (4) and (5) can be written as an <u>*equivalent elastic problem*</u>:

$$\tilde{\boldsymbol{\rho}}\omega^2\mathbf{u}_i = \partial_j\boldsymbol{\sigma}_{ij}\,,\ \text{where}\ \boldsymbol{\sigma}_{ij} = \tilde{\boldsymbol{\lambda}}\boldsymbol{\Delta}\delta_{ij} + 2\tilde{\boldsymbol{\mu}}\boldsymbol{\varepsilon}_{ij}\,, \tag{6}$$

in which the (matrix) parameters of the medium are complex-valued and dependent on ω:

$$\tilde{\boldsymbol{\rho}} = \boldsymbol{\rho} + \frac{i}{\omega}\mathbf{d}\,,\ \tilde{\boldsymbol{\lambda}} = \boldsymbol{\lambda} - i\omega\boldsymbol{\mu}\,,\ \text{and}\ \tilde{\boldsymbol{\mu}} = \boldsymbol{\mu} - i\omega\boldsymbol{\eta}_\mu\,. \tag{7}$$

Transformations (7) give an extended form of the correspondence principle (Lakes, 2009). Importantly, note that the internal friction described by matrix $\mathbf{d}$ modifies the density matrix, making it complex-valued. This is fundamentally different from the conventional viscoelasticity, in which the density always remains real-valued. However, the case $\mathbf{d} \neq \mathbf{0}$ occurs in poroelasticity.

Poroelasticity

With a single internal variable ($N = 1$), zero effective viscosity ($\boldsymbol{\eta} = \mathbf{0}$), and appropriately selected matrices $\boldsymbol{\rho}$, $\mathbf{K}$, $\boldsymbol{\mu}$ and $\mathbf{d}$, the GLS model (3) describes poroelasticity (Biot, 1956). In this case, $\mathbf{u}_0$ represents the deformation of the rock matrix, and the internal variable $\mathbf{u}_1$ can be selected as the filtration displacement (relative coordinate between the fluid and its unperturbed position in host matrix): $\mathbf{u}_1 \equiv \mathbf{u}_{\text{fluid}} - \mathbf{u}_0$. Compared to using $\mathbf{u}_1 \equiv \mathbf{u}_{\text{fluid}}$ in Bourbié et al. (1987), this parameterization simplifies the resulting matrix expressions below. Contributions of solid viscosity ($\boldsymbol{\eta}$ in the second equation (3)) are considered low compared to the friction from the filtration fluid $\mathbf{d}$.

For a simple illustration, let us consider a P wave, in which $\mathbf{u}_0$ and $\mathbf{u}_1$ reduce to the gradients of a scalar potential $\boldsymbol{\Phi}$ (which is, however, a two-component vector in model space): $\mathbf{u} = \nabla\boldsymbol{\Phi}$. The equations of motion (4) become then:

$$\boldsymbol{\rho}\ddot{\boldsymbol{\Phi}} = -\mathbf{d}\dot{\boldsymbol{\Phi}} + \mathbf{R}\nabla^2\boldsymbol{\Phi}\,, \tag{8}$$

where the density, P-wave rigidity, and damping matrices are:

$$\boldsymbol{\rho} = \begin{bmatrix} \rho & \phi\rho_f \\ \phi\rho_f & a\phi\rho_f \end{bmatrix},\ \mathbf{R} = \begin{bmatrix} \lambda_f + 2\mu & M\phi\beta \\ M\phi\beta & M\phi^2 \end{bmatrix},\ \text{and}\ \mathbf{d} = \begin{bmatrix} 0 & 0 \\ 0 & \phi^2\eta/\kappa \end{bmatrix},\ \text{respectively.} \tag{9}$$

In these expressions, λ_f is the Lamé modulus of a closed system (*i.e.* in which the fluid content is constant), $a \geq 1$ is the 'tortuosity', ρ_f is the pore fluid density, and parameter M has the meaning of pressure that needs to be exerted on the fluid in order to increase the fluid content by a unit value at

constant volume (i.e., at $\varepsilon_{kk} = 0$). Parameter $\beta \in [0,1]$ measures the proportion of the apparent macroscopic dilatational strain caused by the variations in fluid content.

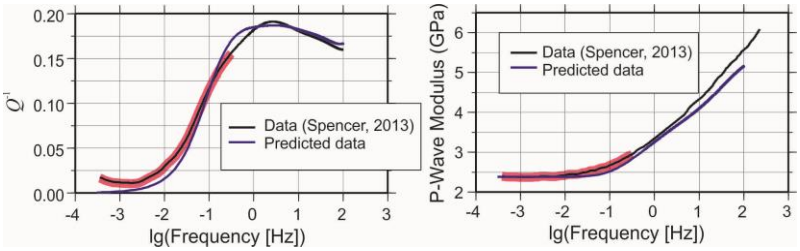

Figure 3. Frequency-dependent Q^{-1} and empirical P-wave modulus of Ells River bitumen sand (Spencer, 2013; black) and GLS models for them (blue; eq. (10)). Pink colour highlights the low-frequency data extrapolated from high-temperature observations (Spencer, 2013).

Example

We consider here only one example of the above model. Black lines in Figure 3 show the empirical P-wave modulus and attenuation Q_{P}^{-1} derived by Spencer (2013) from lab measurements at low frequencies (0.2–205 Hz) and temperature of 5°C. Note that the lower-frequency halves of these curves were inferred from higher-temperature data by using an empirical frequency-temperature relation for polymers (pink in Figure 3; Williams, 1955).

Because the bitumen sand is a compound, its description likely requires internal variables. Modeling a P wave in a GLS medium with a single internal variable fits the data in Figure 3 reasonably well (blue lines in that figure). The parameters of this model are:

$$\boldsymbol{\rho} = \begin{bmatrix} 500 & 3066 \\ 3066 & 4.34 \end{bmatrix} \frac{\mathrm{kg}}{\mathrm{m}^3}, \quad \mathbf{R} = \begin{bmatrix} 2.38 & 24.3 \\ 24.3 & 17.4 \end{bmatrix} \mathrm{GPa}, \quad \boldsymbol{\eta} = \begin{bmatrix} 27.7 & -19.7 \\ -19.7 & 19.7 \end{bmatrix} \mathrm{MPa \cdot s}, \text{ and } \mathbf{d} = \begin{bmatrix} 0 & 0 \\ 0 & 34.3 \end{bmatrix} \frac{\mathrm{kPa \cdot s}}{\mathrm{m}^2}. \quad (10)$$

The structures of these matrices were selected similar to the poroelastic case (9). This is likely not the only plausible solution; however, neither the pure poroelastic model (9) nor the GSLS (Figure 1) explain the bitumen-sand data shown in Figure 3.

Conclusions

A new rheologic model with arbitrary internal variables called the Generalized Linear Solid incorporates fluids, the conventional viscoelastic (Voigt, Maxwell, Burgers, Standard Linear and Generalized Standard Linear) solids, and saturated porous solids. The model successfully predicts the observed behaviour of P waves in bitumen sands, which appear to be neither purely poroelastic nor viscoelastic.

Acknowledgements

This study was supported in part by Canada NSERC Discovery Grant RGPIN261610-03. W. D. was supported by the Scholarship Council, People's Republic of China.

References

Biot, M. A., 1956, Theory of propagation of elastic waves in a fluid-saturated porous solid. I. Low-frequency range. Journal of the Acoustical Society of America 28: 168, doi: 10.1121/1.1908239.

Bourbié, T., O. Coussy, and B. Zinsiger, (1987), Acoustics of porous media. Editions TECHNIP, France, ISBN 2710805168.

Deng, W., and I. B. Morozov, 2013. New approach to finite-difference memory variables by using Lagrangian mechanics, CSEG Convention, http://cseg.ca/resources/abstracts/2013-conference-abstracts-a-to-h, accessed Dec. 22, 2013

Lakes R., 2009. Viscoelastic materials. Cambridge, ISBN 978-0-521-88568-3

Landau, L. and E. Lifshitz, 1986, Theory of elasticity, Pergamon Press, Oxford.

Lines, L., J. Wong, K. Innanen, F. Vasheghani, C. Sondergeld, S. Treitel, and T. Ulrych, 2014, Research Note: Experimental measurements of Q-contrast reflections: Geophysical Prospecting, 62, 190-195, doi: 10.1111/1365-2478.12081.

Liu, H. P., D. L. Anderson, and H. Kanamori, 1976, Velocity dispersion due to anelasticity: implications for seismology and mantle composition, Geophysical Journal of Royal Astronomical Society, 47, 41–58.

Spencer, J. W. 2013. Viscoelasticity of Ells River bitumen sand and 4D monitoring of thermal enhanced oil recovery processes, Geophysics, 78 D419–D428, doi: 10.1190/GEO2012-0535.1

Williams, M. L., R. F. Landel, and J. D. Ferry, 1955, The temperature dependence of relaxation mechanisms in amorphous polymers and other glass forming liquids, Journal of the American Chemical Society, 77, 3701–3707.

Zhu, T., J. M. Carcione, and J.M. Harris, 2013, Approximating constant-Q seismic propagation in the time domain: Geophysical Prospecting, 61, 931 – 940, doi: 10.1111/1365-2478.12044.